Update of the paper investigation

07/25/2019

-- *from June.11th slide* --

Resolving the tensor structure of the Higgs coupling to Z-bosons via Higgs-strahlung

Shankha Banerjee, Rick S. Gupta, Joey Y. Reiness and Michael Spannowsky[1]

[1] *Institute for Particle Physics Phenomenology, Durham University, South Road, Durham, DH1 3LE*

(Dated: May 9, 2019)

arXiv:1905.02728v1 [hep-ph] 7 May 2019

We propose differential observables for $pp \to Z(\ell^+\ell^-)h(bb)$ that can be used to completely determine the tensor structure of the $hZZ^*/hZ\bar{f}f$ couplings relevant to this process in the dimension-6 SMEFT. In particular, we propose a strategy to probe the anomalous $hZ_{\mu\nu}Z^{\mu\nu}$ and $hZ_{\mu\nu}\tilde{Z}^{\mu\nu}$ vertices at the percent level. We show that this can achieved by resurrecting the interference term between the transverse Zh amplitude, which receives contributions from the above couplings, and the dominant SM longitudinal amplitude. These contributions are hard to isolate without a knowledge of the analytical amplitude, as they vanish unless the process is studied differentially in three different angular variables at the level of the Z-decay products. By also including the differential distributions with respect to energy variables, we obtain projected bounds for the two other tensor structures of the Higgs coupling to Z-bosons.

based on an EFT model, can we say something together with our HZZ results ?

Contents of this article is an EFT model

-- Generally speaking, common discussions also found in the other papers/references

II. DIFFERENTIAL ANATOMY OF $pp \to Z(\ell^+\ell^-)h(bb)$ IN THE SMEFT

Including all possible dimension 6 corrections, the most general $hZZ^*/hZ\bar{f}f$ vertex can be parameterised as follows (see for eg. Refs [12, 36, 37])[1],

$$\Delta\mathcal{L}_6^{hZ\bar{f}f} \supset \delta\hat{g}^h_{ZZ}\frac{2m_Z^2}{v}h\frac{Z^\mu Z_\mu}{2} + \sum_f g^h_{Zf}\frac{h}{v}Z_\mu\bar{f}\gamma^\mu f + \kappa_{ZZ}\frac{h}{2v}Z^{\mu\nu}Z_{\mu\nu} + \tilde{\kappa}_{ZZ}\frac{h}{2v}Z^{\mu\nu}\tilde{Z}_{\mu\nu}. \quad (1)$$

the EFT model which generates anomaly coupling at HZZ vertex

$$\sum_{L,R}|\mathcal{A}(\hat{s},\Theta,\theta,\phi)|^2 = a_{LL}\sin^2\Theta\sin^2\theta + a^1_{TT}\cos\Theta\cos\theta + a^2_{TT}(1+\cos^2\Theta)(1+\cos^2\theta) + \cos\varphi\sin\Theta\sin\theta \times (a^1_{LT} + a^2_{LT}\cos\theta\cos\Theta) + \sin\varphi\sin\Theta\sin\theta \times (\tilde{a}^1_{LT} + \tilde{a}^2_{LT}\cos\theta\cos\Theta) + a_{TT'}\cos 2\varphi\sin^2\Theta\sin^2\theta + \tilde{a}_{TT'}\sin 2\varphi\sin^2\Theta\sin^2\theta. \quad (7)$$

signal amplitude has angle dependences

For reference: Coordinate and frames used in this paper

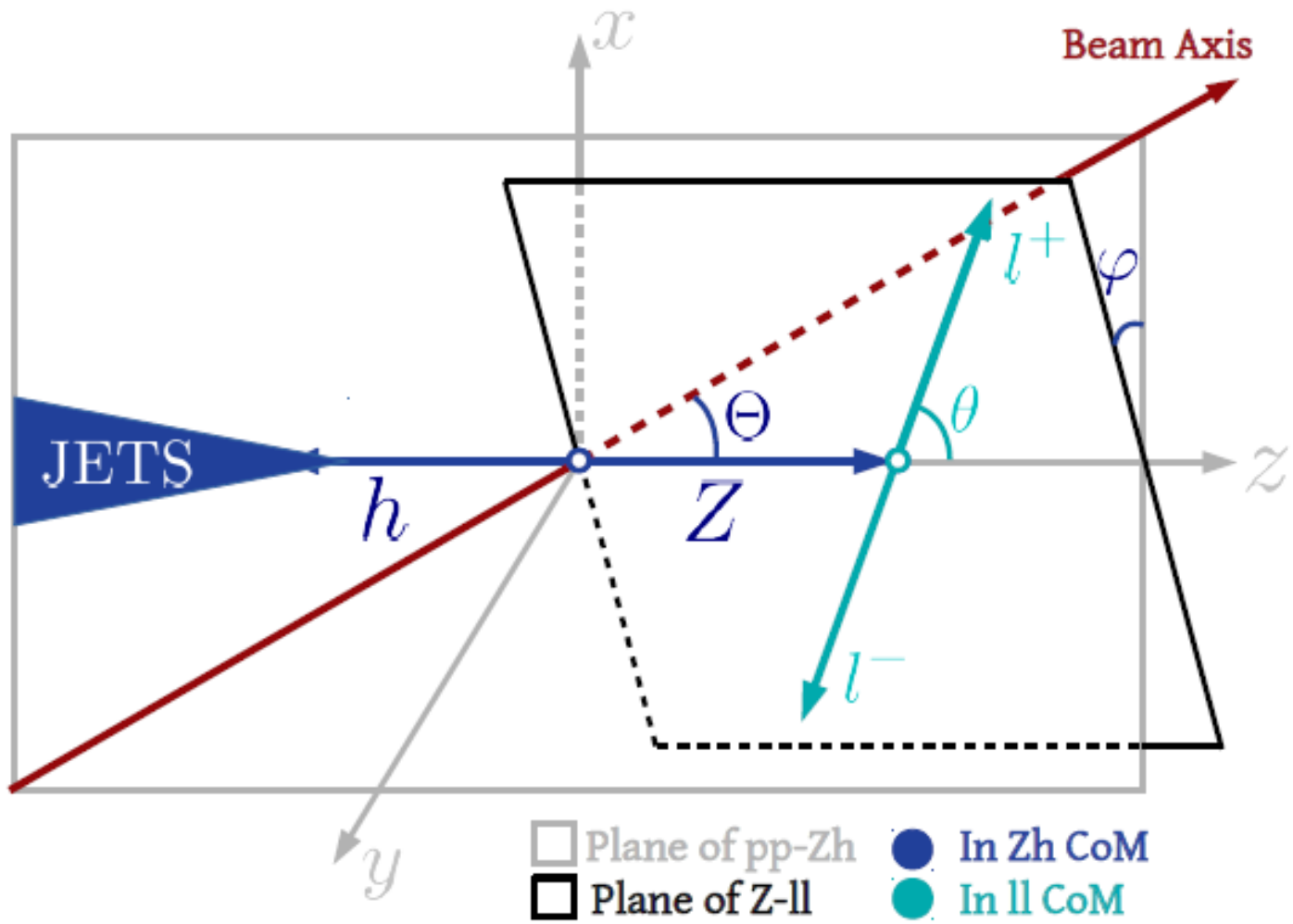

The point I misunderstand is that this HZZ coupling is e^+e^- -> Z*->HZ but not H->ZZ*

・If we look at the CEPC white paper, this study is already included

-- from next page, it is about the while paper & a reference from that

Precision Higgs Physics at the CEPC*

Fenfen An[4,22] Yu Bai[9] Chunhui Chen[22] Xin Chen[5] Zhenxing Chen[3] Joao Guimaraes da Costa[4]
Zhenwei Cui[3] Yaquan Fang[4,6] Chengdong Fu[4] Jun Gao[10] Yanyan Gao[21] Yuanning Gao[3]
Shao-Feng Ge[15,28] Jiayin Gu[13] Fangyi Guo[1,4] Jun Guo[10,11] Tao Han[5,30] Shuang Han[4]
Hong-Jian He[10,11] Xianke He[10] Xiao-Gang He[10,11] Jifeng Hu[10] Shih-Chieh Hsu[31] Shan Jin[8]
Maoqiang Jing[4,7] Ryuta Kiuchi[4] Chia-Ming Kuo[20] Pei-Zhu Lai[20] Boyang Li[5] Congqiao Li[3] Gang Li[4]
Haifeng Li[12] Liang Li[10] Shu Li[10,11] Tong Li[12] Qiang Li[3] Hao Liang[4,6] Zhijun Liang[4]
Libo Liao[4] Bo Liu[4,22] Jianbei Liu[1] Tao Liu[14] Zhen Liu[25,29] Xinchou Lou[4,6,32] Lianliang Ma[12]
Bruce Mellado[17,18] Xin Mo[4] Mila Pandurovic[16] Jianming Qian[23] Zhuoni Qian[19]
Nikolaos Rompotis[21] Manqi Ruan[4] Alex Schuy[31] Lian-You Shan[4] Jingyuan Shi[9] Xin Shi[4]
Shufang Su[24] Dayong Wang[3] Jing Wang[4] Lian-Tao Wang[26] Yifang Wang[4,6] Yuqian Wei[4]
Yue Xu[5] Haijun Yang[10,11] Weiming Yao[27] Dan Yu[4] Kaili Zhang[4,6] Zhaoru Zhang[4]
Mingrui Zhao[2] Xianghu Zhao[4] Ning Zhou[10]

[1] Department of Modern Physics, University of Science and Technology of China, Anhui 230026, China
[2] China Institute of Atomic Energy, Beijing 102413, China
[3] School of Physics, Peking University, Beijing 100871, China
[4] Institute of High Energy Physics, Beijing 100049, China
[5] Department of Engineering Physics, Physics Department, Tsinghua University, Beijing 100084, China
[6] School of Physical Sciences, University of Chinese Academy of Science (UCAS), Beijing 100049, China
[7] School of Nuclear Science and Technology, University of South China, Hengyang 421001, China
[8] Department of Physics, Nanjing University, Nanjing 210093, China
[9] Department of Physic Southern Eastern University, Nanjing 210096, China
[10] School of Physics and Astronomy, Shanghai Jiao Tong University, KLPPAC-MoE, SKLPPC, Shanghai 200240, China
[11] Tsung-Dao Lee Institute, Shanghai 200240, China
[12] Institute of Frontier and Interdisciplinary Science and Key Laboratory of Particle Physics and Particle Irradiation (MOE), Shandong University, Qingdao 266237, China
[13] PRISMA Cluster of Excellence & Mainz Institute of Theoretical Physics, Johannes Gutenberg-Universität Mainz, Mainz 55128, Germany
[14] Department of Physics, Hong Kong University of Science and Technology, Hong Kong
[15] Kavli IPMU (WPI), UTIAS, The University of Tokyo, Kashiwa, Chiba 277-8583, Japan
[16] Vinca Institute of Nuclear Sciences, University of Belgrade, Belgrade 11000, Serbia
[17] School of Physics and Institute for Collider Particle Physics, University of the Witwatersrand, Johannesburg 2050, South Africa
[18] iThemba LABS, National Research Foundation, PO Box 722, Somerset West 7129, South Africa
[19] Center for Theoretical Physics of the Universe, Institute of Basic Science, Daejeon 34126, South Korea
[20] Department of Physics and Center for High Energy and High Field Physics, National Central University, Taoyuan City 32001, Taiwan
[21] Department of Physics, University of Liverpool, Liverpool L69 7ZX, United Kingdom
[22] Department of Physics and Astronomy, Iowa State University, Ames 50011-3160, USA
[23] Department of Physics, University of Michigan, Ann Arbor, Michigan 48109, USA
[24] Department of Physics, University of Arizona, Arizona 85721, USA
[25] Theoretical Physics Department, Fermi National Accelerator Laboratory, Batavia 60510, USA
[26] Department of Physics, University of Chicago, Chicago 60637, USA
[27] Lawrence Berkeley National Laboratory, Berkeley, California 94720, USA
[28] Department of Physics, University of California, Berkeley, California 94720, USA
[29] Maryland Center for Fundamental Physics, Department of Physics, University of Maryland, College Park, Maryland 20742, USA
[30] Department of Physics & Astronomy, University of Pittsburgh, Pittsburgh 15260, USA
[31] Department of Physics, University of Washington, Seattle 98195-1560, USA
[32] Department of Physics, University of Texas at Dallas, Texas 75080-3021, USA

Abstract: The discovery of the Higgs boson with its mass around 125 GeV by the ATLAS and CMS Collaborations marked the beginning of a new era in high energy physics. The Higgs boson will be the subject of extensive studies

Received XX August XXXX

* Supported by the National Key Program for S&T Research and Development (2016YFA0400400); CAS Center for Excellence in Particle Physics; Yifang Wangs Science Studio of the Ten Thousand Talents Project; the CAS/SAFEA International Partnership Program for Creative Research Teams (H751S018S5); IHEP Innovation Grant (Y4545170Y2); Key Research Program of Frontier Sciences, CAS (XQYZDY-SSW-SLH002); Chinese Academy of Science Special Grant for Large Scientific Project (113111KYSB20170005); the National Natural Science Foundation of China(11675202); the Hundred Talent Programs of Chinese Academy of Science (Y3515540U1); the National 1000 Talents Program of China; Fermi Research Alliance, LLC (DE-AC02-07CH11359); the NSF under Grant No. PHY1620074

Constraints on the top-quark and bottom-quark Yukawa couplings, including their CP phases, are presented, respectively, in the left and right panels of Fig. 24, respectively. The 68% and 95% CL exclusion bands are shown in solid and dashed lines. The limits for the CEPC are shown in *bright* black and magenta lines for individual operator analysis and the *bright* green and yellow shaded regions representing the allowed parameter space at 68% and 95% CL, respectively. The *dimmed* thick black curves represent the results after turning on both operators $\mathcal{O}_{ut}$ and $\mathcal{O}_{bt}$ at the same time, using a profile-likelihood method profiling over other parameters. Furthermore, in the left panel the cyan band represents constraints from the HL-LHC $t\bar{t}H$ measurements, red bands are constraints from the CEPC $H \to gg$ measurements and blue bands are constraints from the CEPC $H \to \gamma\gamma$ measurements. Similarly, in the right panel, the cyan bands are constraints from $H \to b\bar{b}$ and the red bands are constraints from $H \to gg$ at the CEPC.

The left panel of Fig. 24 shows that the expected sensitivity on the modification in the magnitude of top-quark Yukawa coupling is around $\pm 3\%$ for the single operator analysis. This is relaxed to $[-9.5\%, +3\%]$ assuming zero CP phase for the top-quark Yukawa coupling and allowing the bottom-quark Yukawa coupling and its phase to vary freely. The phase of the top-quark Yukawa coupling can be constrained to $\pm 0.16\pi$. This constraint is driven by the $H \to \gamma\gamma$ measurement, where a sizable phase shift will enlarge the $H \to \gamma\gamma$ decay rate via reducing the interference with the SM W boson loop. The constraint on the magnitude of the top-quark Yukawa coupling is driven by the $H \to gg$ measurement which is dominated by the top-quark loop contribution. Note that constraints from the $H \to gg$ measurement are not constant with respect to the Yukawa coupling magnitude. This is due to the different sizes of the top-quark loop contribution to Hgg through scalar and pseudoscalar couplings. Similarly, as shown in the right panel of Fig. 24 for the bottom-quark Yukawa coupling, the constraint for the magnitude is $\pm 2.5\%$. For the CP phase, the constraint changes from $\pm 0.47\pi$ to zero when the top-quark Yukawa coupling is left free.

8 Higgs boson CP test and exotic decays

In addition to the studies based on the simulation of the CEPC baseline conceptual detector, the sensitivity of tests on Higgs boson spin/CP properties and in constraining branching ratios of Higgs boson exotic decays are also estimated. These estimates are based on previously published phenomenological studies and are summarized in this section.

8.1 Tests of Higgs boson spin/CP property

The CP properties of the Higgs boson and, more generally, its anomalous couplings to gauge bosons in the presence of BSM physics, can be measured at the CEPC using the $e^+e^-(\to Z^*) \to ZH \to \mu^+\mu^- b\bar{b}$ process. It is convenient to express the effects of the anomalous couplings in terms of the fractions of events from the anomalous contribution relative to the SM predictions. These fractions are invariant under the independent rescalings of all couplings, see Refs. [128–130].

Two of the anomalous HZZ coupling measurements are of particular interest at the CEPC: the fraction of the high-order CP-even contribution due to either SM contribution or new physics, f_{a2}, and the fraction of a CP-odd contribution due to new physics, f_{a3}. The following two types of observables can be used to measure these anomalous couplings of the Higgs bosons.

1. The dependence of the $e^+e^- \to Z^* \to ZH$ cross section on $\sqrt{s}$ is different for different CP property of the Higgs boson [130]. Therefore, measurements of the cross section at several different energies will yield useful information about anomalous HZZ couplings. However this has non-trivial implications to the accelerator design and is not included in this study as a single value of $\sqrt{s}$ is assumed for the CEPC operating as a Higgs boson factory.

2. Angular distributions, $\cos\theta_1$ or $\cos\theta_2$ and Φ as defined in Fig. 25. These angles are also sensitive to interference between CP-even and CP-odd couplings. In particular forward-backward asymmetry with respect to $\cos\theta_1$ or $\cos\theta_2$ and non-trivial phase in the Φ distributions can lead to an unambiguous interpretation of CP violation.

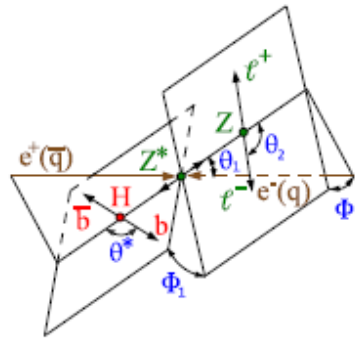

Fig. 25. The Higgs boson production and decay angles for the $e^+e^- \to Z^* \to ZH \to \mu^+\mu^- b\bar{b}$ process [130].

From the reference in the white paper :

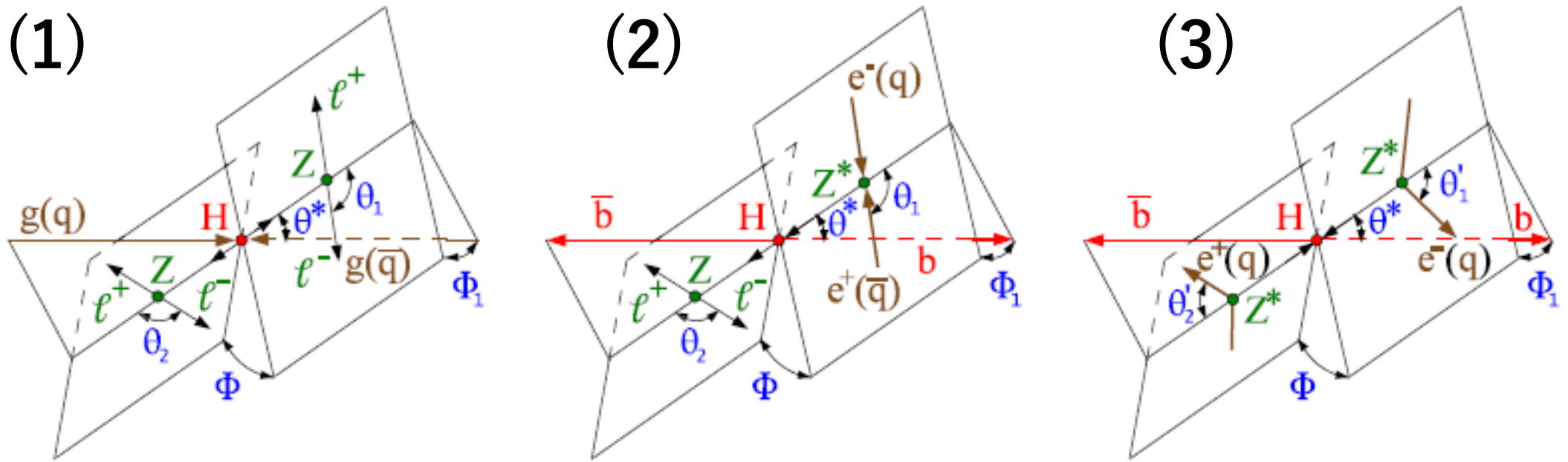

FIG. 1: Illustrations of H particle production and decay in pp or e^+e^- collision $gg/q\bar{q} \to H \to ZZ \to 4\ell^\pm$ (left), $e^+e^-(q\bar{q}) \to Z^* \to ZH \to \ell^+\ell^- b\bar{b}$ (middle), or $e^+e^-(qq') \to e^+e^-(qq')H \to e^+e^-(qq')b\bar{b}$ (right). The $H \to b\bar{b}$ decay and HZZ coupling are shown as examples, so that Z can be substituted by other vector bosons. Five angles fully characterize the orientation of the production and decay chain and are defined in the suitable rest frames.

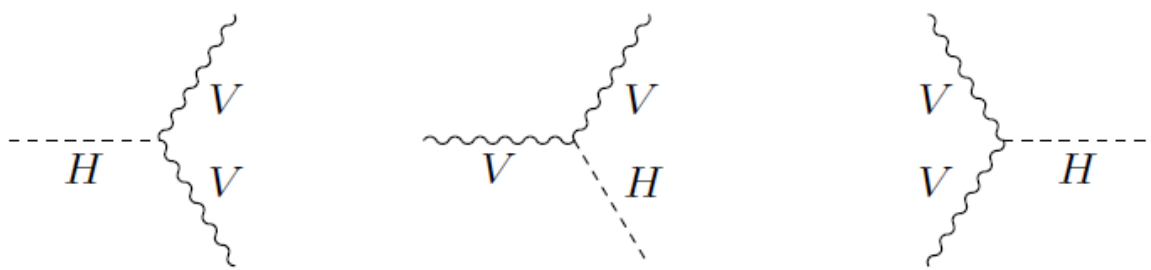

1. The $H \to VV^*$ process

We begin by describing the decay process $H \to VV \to 4f$, following notation of Refs. [7, 8]. This process is important not only because it can be used directly to constrain anomalous couplings but also because various crossings of $H \to VV$ amplitude give amplitudes for associated Higgs boson production and vector boson fusion. Complete description of the decay amplitude for $H \to VV^*$ requires two invariant masses and five angles, defined in Fig. 1. We collectively denote these angles as $\vec{\Omega} = (\cos\theta^*, \Phi_1, \cos\theta_1, \cos\theta_2, \Phi)$. The probability distribution that describes the decay of a Higgs boson to two gauge bosons V is written as

$$\frac{d\Gamma(m_1, m_2, \vec{\Omega})}{dm_1\, dm_2\, d\vec{\Omega}} \propto |\vec{p}_V(m_1, m_2)| \times \frac{m_1^3}{(m_1^2 - m_V^2)^2 + m_V^2\Gamma_V^2} \times \frac{m_2^3}{(m_2^2 - m_V^2)^2 + m_V^2\Gamma_V^2} \times \frac{d\Gamma(m_1, m_2, \vec{\Omega})}{d\vec{\Omega}}, \quad \text{(A1)}$$

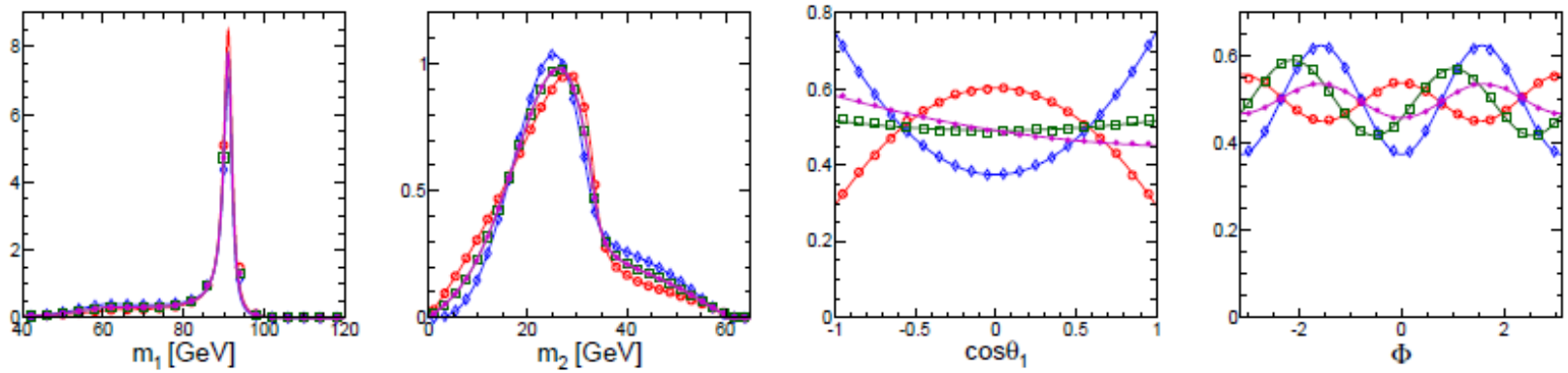

FIG. 14: Distributions of the observables in the $H \to ZZ$ analysis, from left to right: m_1, m_2 (where $m_1 > m_2$), $\cos\theta_1$ (same as $\cos\theta_2$), and Φ. Points show simulated events and lines show projections of analytical distributions. Four scenarios are shown: SM (0^+, red open circles), pseudoscalar (0^-, blue diamonds), and two mixed states corresponding to $f_{a3} = 0.5$ with $\phi_{a3} = 0$ (green squares) and $\pi/2$ (magenta points). For a spin-zero particle, distributions in $\cos\theta^*$ and Φ_1 are trivially flat, but this is not true for higher-spin states [8] or with detector effects.

Comments

・ the study at the ILC (for example, arXiv: 1712.09772v1) or presentation by Fadol on workshop @PKU (https://indico.ihep.ac.cn/event/9832/session/9/contribution/20/material/slides/0.pdf)
utilizes the ee->Z*->ZH vertex , but not ee->Z*->ZH->ZH(->ZZ) vertex.

probably due to the difference of statistics and so on.

(my personal feeling is that ...) Can we still perform the differential analysis ?
I mean , for example, ee->Z*->ZH->ZH(->ZZ) has two HZZ vertices, can we do something with that , though the statistics would be the clear problem.